FORUM GEOGRAFI
ISSN: 0852-0682 | E-ISSN: 2460-3945

HTTPS://JOURNALS.UMS.AC.ID/INDEX.PHP/FG/

Research article

Linking Weather Variability and Wildfires Across Tropical Ecoregions: Evidence from Sumatra, Indonesia

Asshaffa Naim[1], Andung Bayu Sekaranom[2,*], Sudrajat[2], Fitria Nucifera[3]

[1] Master in Geography Program, Faculty of Geography, Universitas Gadjah Mada, 55281, Yogyakarta, Indonesia; [2] Department of Environmental Geography, Faculty of Geography, Universitas Gadjah Mada, 55281, Yogyakarta, Indonesia; [3] Division of Sustainable Energy and Environment, Graduate School of Engineering, The University of Osaka, 565-0871, Osaka, Japan.

[*)] Correspondence: andung.geo@ugm.ac.id

Citation:

Naim, A., Sekaranom, A. B., Sudrajat, & Nucifera, F. (2026). Linking Weather Variability and Wildfire Across Tropical Ecoregions: Ev-idence from Sumatra, Indonesia. Forum Geografi. 40(3), 391-406.

Article history:
Received: 24 February 2026
Revised: 1 July 2026
Accepted: 1 July 2026
Published: 6 July 2026

Abstract

Wildfires in tropical regions exhibit strong spatial variability that reflects differences in ecoregion characteristics and weather sensitivity. This study aims to examine the relationship between weather dynamics and wildfire distribution across six different ecoregion characteristics in Sumatra. MODIS Fire hotspot data were used to analyze wildfire distribution from 2016–2023, combined with ERA5 and SMAP soil moisture data. Negative binomial regression and incidence rate ratio analysis were performed to obtain a statistical measure of the influence of weather. The results show that wildfire occurrence was highly concentrated in coastal and swamp ecoregions, with peat swamp forests (PSFs) accounting for the highest hotspot density. Pre-fire weather analyses showed that swamp and mangrove ecoregions exhibited higher sensitivity to relatively small rainfall deficits and temperature increases compared to upland forests. The negative binomial regression indicated that the strongest weather–wildfire associations were in freshwater swamp forest (FSFs), where weather variables yielded the highest pseudo-R^2 (0.226). The distinct weather sensitivity of each ecoregion was further explained by the IRR values, which showed strong temperature sensitivity in the Sunda Shelf mangrove (SSM) region and a prominent rainfall-related suppression of wildfire activity in FSFs. The findings demonstrate ecoregion-specific wildfire sensitivity and the need for targeted wildfire management strategies, particularly in peatland and coastal ecosystems in Sumatra.

Keywords: ecoregion; wildfire; Sumatra; precipitation; temperature; soil moisture.

1. Introduction

Global warming has increased wildfire vulnerability by increasing temperatures and reducing precipitation levels, a situation which creates dry and flammable environmental conditions (Gincheva *et al.,* 2024). Wildfires, such as those in Australia during the 2019-2020 season, have burned approximately 3-4% of the world's land area, causing extensive ecosystem damage and producing large amounts of greenhouse gas emissions (Chen & Liu, 2024; Nolan *et al.,* 2020). These incidents are driven by a combination of dry weather conditions and human activities, such as land clearing, agriculture and deforestation (Liu *et al.,* 2024). Weather dynamics, particularly declining precipitation and rising temperatures, have been known to increase the number of wildfires by facilitating evapotranspiration and reducing fuel moisture (Cho *et al.,* 2024; Wasserman & Mueller, 2023). Several studies have shown that the influence of weather variability on wildfire activity is strongly mediated by the characteristics of soil, vegetation, hydrology and climate within an ecoregion (Moradi & Rahmati, 2023). Consequently, the distribution patterns vary across ecoregion types, making ecoregion-based analysis essential for understanding the mechanisms of wildfire occurrence and providing an ecologically grounded framework for understanding ecological sensitivity to wildfire. Addressing this variability requires spatially explicit evidence and analytical approaches that can capture related heterogeneity.

Satellite products such as MODIS and VIIRS enable near real-time detection of fire-prone locations through hotspot identification based on thermal anomaly algorithms (Briones-Herrera *et al.,* 2020). These hotspot datasets serve as proxies for wildfire occurrence, which, when combined with weather and soil conditions, allow for a comprehensive assessment of sensitivity across ecoregions. The use of negative binomial regression further strengthens analysis by quantifying the relationship between wildfire frequency and weather dynamics, while addressing overdispersion in hotspot data. By integrating satellite-based hotspot detection with reanalysis of climate and soil moisture data through an ecoregion-based statistical framework, this study not only contributes to advancing scientific understanding of wildfire–weather interactions in tropical landscapes, but also points to practical implications for early warning systems and management policies. Integrating ecoregion-specific weather sensitivity into prevention planning can enhance both short-term preparedness and long-term adaptation, thereby reducing ecological degradation and public health risks associated with recurrent wildfires.

Previous tropical wildfire studies have predominantly focused on large-scale climate variability, such as ENSO and IOD, as primary drivers of interannual wildfire variability across Southeast Asia (Brasika, 2022; Novitasari *et al.,* 2019; Nurdiati *et al.,* 2022). Subsequent studies have incorporated local hydrological controls, peatland characteristics, and human-induced landscape modifications to improve risk assessment (Salmayenti *et al.,* 2025; Taufik *et al.,* 2022). Recently, machine learning approaches and fire danger models have been applied to evaluate spatial patterns of susceptibility under varying climatic conditions (Hayasaka, 2023; Prasetyo et al., 2022), while broader studies have documented the emergence of novel fire regimes across tropical forests worldwide (Li *et al.,* 2025; Pacuk *et al.,* 2025). Despite these advances, the role of ecoregional characteristics in shaping wildfire responses to short-term weather variability remains insufficiently understood. Previous studies generally focus on specific ecosystem, particularly peatlands, or assess fire-weather relationships at broad spatial scales without considering ecological heterogeneity among landscapes. Consequently, it remains unclear whether similar short-term weather anomalies exert comparable influences on wildfire occurrence across different ecoregions, or whether ecological characteristics modulate the magnitude and direction of these relationships (Quan *et al.,* 2023). This knowledge gap limits the ability to identify ecosystem-specific drivers and constrains the development of differentiated wildfire mitigation strategies.

To address this gap, this study was conducted to investigate wildfire-triggering weather conditions from an ecoregion perspective. Rather than treating tropical landscapes as environmentally homogeneous, the study examines whether the sensitivity of wildfire occurrence to short-term prefire weather variability differs systematically among distinct ecoregion types in Sumatra. By integrating MODIS FIRMS hotspot observations, ERA5 weather variables, and SMAP soil moisture data within an ecoregion-based statistical framework, the results quantify and compare fire-weather relationships across multiple tropical ecosystems simultaneously. Therefore, the study aims to 1) describe the spatial and temporal distribution of hotspots based on ecoregions; 2) analyze the spatial and temporal dynamics of precipitation, temperature and soil moisture before the emergence of hotspots; and 3) assess the relationship between hotspots and variability in precipitation, temperature and soil moisture. This approach will provide new insights into how ecological characteristics mediate wildfire responses to weather anomalies, advancing a more ecosystem-specific understanding of wildfire processes in tropical regions.

2. Methods

The study framework comprised four sequential stages: data acquisition, data pre-processing, spatial and temporal analysis, and statistical analysis. A detailed workflow is presented in Figure 1. The methodological approach shared conceptual similarities with recent wildfire–weather analyses in other tropical and subtropical regions, yet differed in several key respects. For instance, studies in semi-arid tropical regions have used monthly or seasonal weather aggregates (Justino *et al.,* 2023), while our study used daily pre-fire windows to capture short-term atmospheric triggers. In addition, unlike analyses that treat entire islands as single analytical units (Nurdiati *et al.,* 2022), this study stratified observations by ecoregion to enable finer ecological differentiation. The integration of SMAP soil moisture alongside ERA5 data also distinguishes this framework from other studies which have relied solely on precipitation-based indices to address the need for multivariable fire risk modelling (Krueger *et al.,* 2022; Quan *et al.,* 2023).

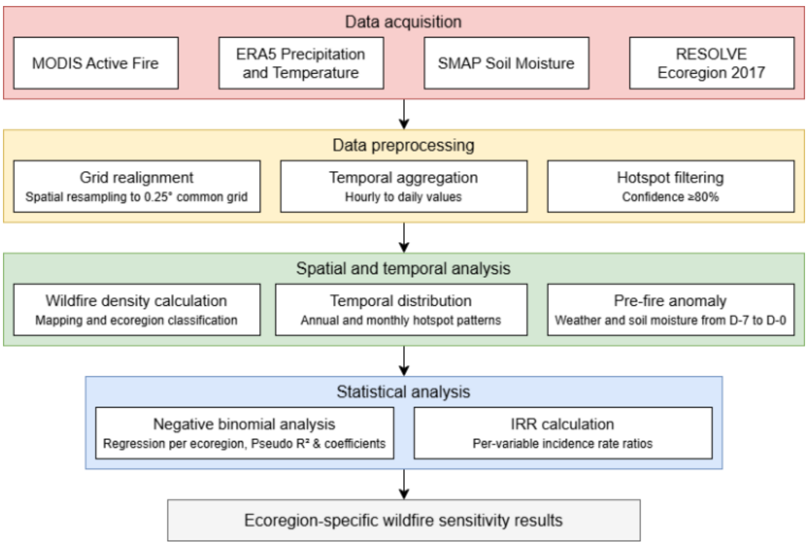

Figure 1. Study Framework (Source: Methodological Review).

2.1. Study Area

The study area was the island of Sumatra in Indonesia, with a total area of 448,975 km^2, spanning 95°0′35″ to 106°11′22″ east and 5°56′36″ south to 6°4′37″ north. The island stretches from northwest to southeast, and is located southwest of the Malay Peninsula, bordered by the Indian Ocean to the west and east, and the Malacca Strait and South China Sea to the east. Topographically, it is characterized by mountainous terrain in its western and northern regions, while the eastern region is dominated by extensive lowlands. In addition, it has a tropical climate with two main seasonal patterns: an equatorial type with two rainfall peaks in the northern and central parts; and a monsoonal type with a single rainfall peak in the southern region (Ariska et al., 2024). Figure 2 shows that the study area covers six ecoregions based on biogeographical and ecological characteristics proposed by Dinerstein *et al.* (2017), consisting of tropical pine forest (TPF), montane rainforest (MRF), lowland rainforest (LRF), freshwater swamp forest (FSF), peat swamp forest (PSF), and Sunda Shelf mangrove (SSM) areas.

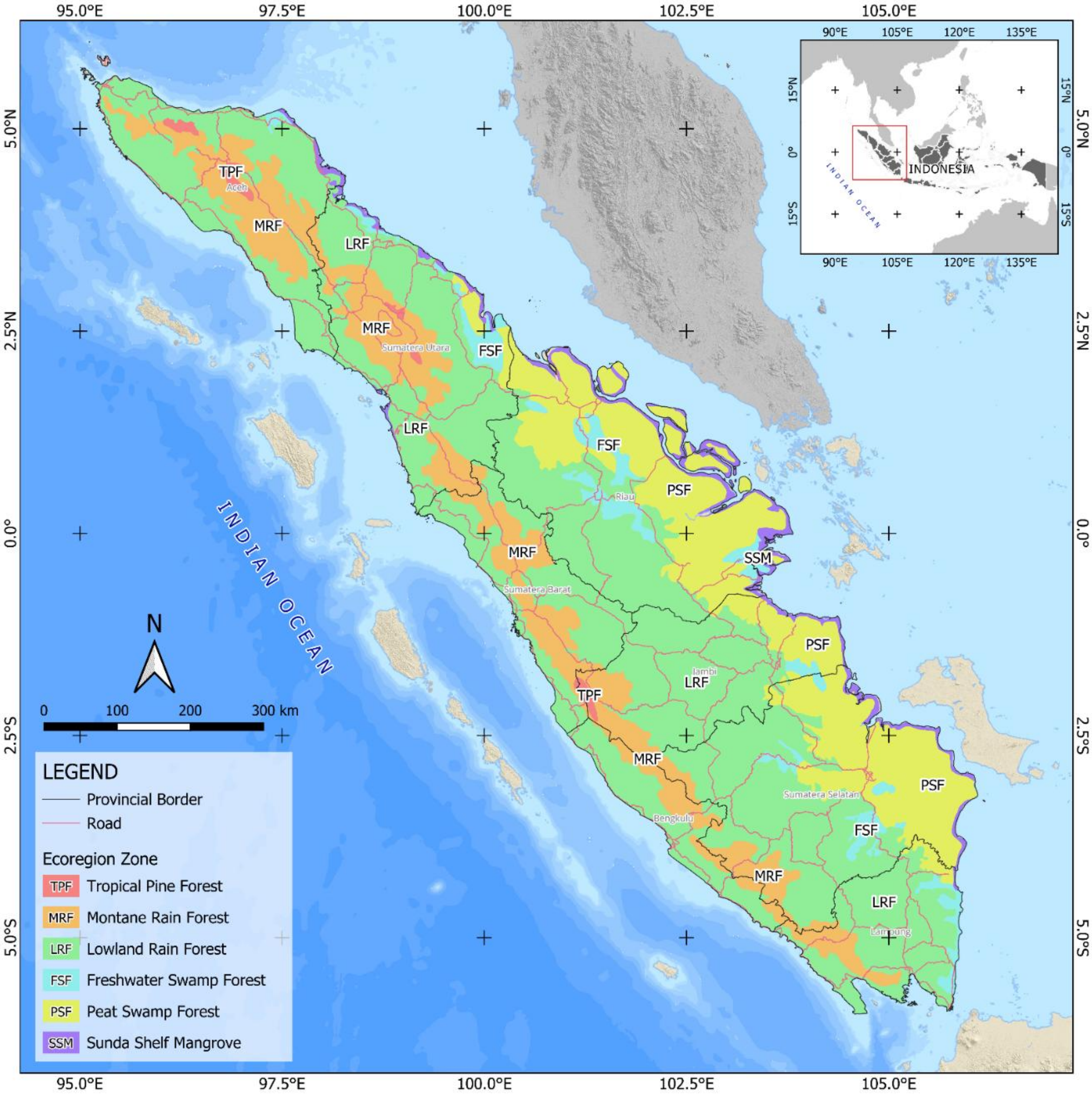

Figure 2. Study Area (Source: Data Processing in QGIS 3.34).

Sumatra is one of the most critical regions in Indonesia for study of the link between weather variability and wildfire hotspots across ecoregions. Over the past decade, more than 2.8 million ha of land have burned on the island (Kementerian Kehutanan, 2025). Sumatra hosts the largest peatland area in the country, covering approximately 6.4 million hectares, primarily in Riau, Jambi and South Sumatra (Ritung *et al.,* 2018). Peatland is highly vulnerable to wildfires because of its high organic content, which becomes extremely flammable under dry conditions, especially during prolonged droughts often triggered by global climate phenomena such as El Niño (Hayasaka, 2023). Sumatra is also home to endangered and endemic species, which encounter heightened threats from recurring wildfires. Evidence shows that species diversity indices in burned forests are significantly lower than in unburned areas (Syaufina *et al.,* 2018). Due to this combination of weather sensitivity and ecological importance, Sumatra provides a critical setting for analyzing how weather variability shapes wildfire occurrence across ecoregions.

The study spanned eight years (2016-2023), a period selected to capture significant interannual climate variability, including both relatively wet and dry years, and to ensure temporal consistency across all datasets. The period was selected for several other reasons. First, the SMAP satellite became fully operational in April 2015, making 2016 the first complete calendar year with consistently available soil moisture data across all three datasets. Second, the period comprised marked interannual climate variability, including strong El Niño years and near-normal conditions, which allowed robust statistical analysis. Finally, the MODIS and ERA5 data for 2024 onwards were incompletely processed in the accessible repositories at the time of the analysis.

2.2. Datasets

Four primary datasets were used, consisting of wildfire data, weather data, soil moisture data and ecoregion data. Each was downloaded using a common bounding box (7°S-7°N, 94°E-107°E) to ensure complete spatial coverage of the study area and consistent data processing. Wildfire data were in the form of fire hotspot locations, sourced from the MODIS Active Fire Product and accessed through NASA FIRMS (firms.modaps.eosdis.nasa.gov) (Giglio *et al.,* 2016). This dataset was generated from the identification of wildfire hotspots in MODIS imagery, based on a series of algorithms and thresholds that had been adjusted to local conditions (Giglio *et al.,* 2016). Each hotspot represented a thermal anomaly and indicated relative wildfire activity patterns rather than exact wildfire extent or perimeters. MODIS also provided a confidence value that represented the likelihood that a detected hotspot corresponded to an actual wildfire event. This feature served to filter the data and retain only high-confidence hotspots, which reduced false detections and improved the reliability of regional-scale wildfire pattern analysis.

Weather data were represented by precipitation and temperature variables taken from the ERA5 datasets, a global weather parameter dataset that combines model output with observation data to provide temporally consistent climate variables, which is widely used to analyze long-term trends in climatic studies (Sabljić *et al.,* 2026). Daily total precipitation and 2m temperature data were obtained from the ERA5 reanalysis dataset (cds.climate.copernicus.eu) at a spatial resolution of 0.25° × 0.25° and hourly temporal resolution for the period 2016 to 2023 (Hersbach *et al.,* 2023). These variables were selected as fundamental drivers of wildfire risk. Temperature directly influences the rate of evapotranspiration, which dries out vegetation and other potential fuels, thereby leading to more flammable conditions (Wasserman & Mueller, 2023). Precipitation is the primary source of moisture for both live and dead fuels, with its absence or scarcity being a direct indicator of drought conditions conducive to fire ignition and spread (Cho *et al.,* 2024; Lafon & Quiring, 2012).

Soil moisture data were sourced from SMAP Surface and Root Zone Soil Moisture (appears.earthdatacloud.nasa.gov) at a spatial resolution of approximately 9 km and a 3-hourly temporal resolution (Reichle *et al.,* 2022). This variable was selected because it provides a more stable and integrated measure of landscape dryness than precipitation alone. In addition, it shows the cumulative effect of past rainfall and temperature, which indicates overall water stress on vegetation and the moisture content of deeper organic soil layers, crucial in peatland wildfire analysis (Krueger *et al.,* 2022). Building on this landscape-specific approach, the RESOLVE Ecoregions 2017 dataset was used to delineate distinct ecological zones for a stratified analysis (ecoregions.appspot.com) (Dinerstein *et al.,* 2017). The ecoregion represented broad biogeographical and ecological characteristics that were appropriate for capturing underlying climatic, hydrological and ecological controls, shaping long-term wildfire sensitivity across landscapes. While land use and land cover (LULC) change occurred, the ecoregion provided a more stable and ecologically meaningful basis than the dynamic land cover classes (Curcan *et al.,* 2023; Drăguleasa *et al.,* 2023; Măceșeanu *et al.,* 2026), especially given the island-wide scale of the study.

2.3. Data Processing

All the variables were resampled to a common 0.25° grid corresponding to the ERA5 resolution using bilinear interpolation that estimated values at target grid points by computing a weighted average of the four nearest source grid cells to ensure spatial consistency across datasets. This resulted in approximately 2200 grid cells covering Sumatra. Temporally, ERA5 hourly data and SMAP 3-hourly data were aggregated to daily values by computing the daily means. Data processing and spatial analysis were conducted using QGIS version 3.34.12, while statistical analyses were performed using Python (including xarray, numpy and geopandas libraries) (Arias-Muñoz *et al.,* 2024; Prasetyo *et al.,* 2022). Raw hotspot data from MODIS were filtered to minimize false detections. Only hotspots with a confidence value > 80% were retained, following the high-confidence threshold recommended in the product's user guide (Giglio *et al.,* 2016). Subsequently, these filtered points were aggregated to calculate fire density within the common grid. In addition to density calculations, the plotted hotspots were also classified based on their zones. Annual and monthly wildfire accumulation in each ecoregion was also calculated for temporal analysis.

For each hotspot, the corresponding weather and soil moisture data were extracted for the seven days preceding each hotspot detection, denoted as D-7 to D-0 to represent the pre-fire period. This window was selected based on previous studies that have consistently identified 5- to 10-day antecedent drying periods as the most critical precursors to fire ignition, with soil moisture and atmospheric dryness responding most strongly to rainfall deficits within this timeframe (Chowdhury & Hassan, 2015; Quan *et al.,* 2023). In addition, the lag time between rainfall cessation and critical near-surface moisture depletion in tropical peatlands have typically fallen within a 3-7 day range (Taufik *et al.,* 2022). This confirmed its suitability as the optimal temporal resolution for capturing short-term wildfire conditioning in the study context. The daily average value of each variable was calculated for each grid cell, while anomalies were calculated as the difference between the daily observed value and the pre-fire period mean across all hotspot events, as a standardized measure of departure from the pre-fire baseline condition. The processed hotspot densities and variables were analyzed on both monthly and annual scales. Data were classified and aggregated based on their ecoregion zones to facilitate a comparative analysis of wildfire dynamics.

2.4. Statistical Analysis

Wildfire occurrences referred to count data that typically exhibited overdispersion, a scenario in which the variance in the data is significantly larger than the mean. This was common because many grid cells had zero wildfires, while a few exhibited a very high concentration. Therefore, to quantify the relationship between environmental conditions and wildfire occurrence, a negative binomial regression model was used. This statistical method was chosen to address wildfire data overdispersion. The appropriateness of the negative binomial model over Poisson regression was evaluated by testing the statistical significance of the dispersion parameter (α); a statistically significant α ($p < 0.05$) indicated the presence of overdispersion. The negative binomial model was a more robust and valid choice as it included an extra variable to account for this excess variance (Stoklosa *et al.,* 2022). The regression model was formally expressed as Equation 1:

$$log(\mu_i) = \beta_0 + \beta_1 \cdot P_i + \beta_2 \cdot T_i + \beta_3 \cdot SM_i + \varepsilon_i \quad (1)$$

where μ_i represents the expected number of high-confidence hotspots in grid cell i; P, T and SM show the 7-day pre-fire mean values of precipitation (mm), temperature (°C) and soil moisture (%) respectively; β_0 is the intercept; β_1, β_2, and β_3 are the estimated regression coefficients; and ε_i is the error term. The model incorporated a dispersion parameter α that allowed variance to exceed the mean, thereby addressing the overdispersion inherent in hotspot count data.

The statistical significance of the predictor variables within the negative binomial regression was evaluated at a 95% confidence level (p-value < 0.05). Variables yielding a p-value of less than 0.05 were considered statistically significant drivers of fire occurrence. In the model, the number of high-confidence hotspots per grid cell served as the dependent variable. The 7-day pre-fire averages of temperature, precipitation and soil moisture were used as the independent (predictor) variables, and the statistical analysis was performed for each ecoregion and for the whole region. Negative binomial analysis for the MRF and TPF ecoregions was conducted simultaneously because the number of hotspots in the TPF did not meet the minimum number of units. The results of this regression were presented in a table that included the pseudo-R2 variable, regression coefficients, and incidence rate ratio (IRR) values. Pseudo-R^2 measured the improvement in model fit of the full model relative to a null (intercept-only) model, in which higher values indicated a stronger association between the predictor variables and wildfire occurrence. Significance and coefficients indicated influential variables, while IRR described the magnitude of that influence on wildfire occurrence (Piza, 2012).

3. Results

3.1. Spatial and Temporal Wildfire Distribution

The distribution of 19,450 hotspots recorded during the period 2016-2023 on Sumatra Island, as shown in Figure 3, revealed a concentration in the eastern region of the island, especially in the PSF ecoregion. Hotspots were aggregated within 0.25° grid cells, resulting in an average hotspot density of 28.85 points per grid cell. The maximum count within a single cell reached 1,222 hotspots, while 170 cells contained none. The highest number of hotspots was found in the PSF ecoregion, with 11,936 and a density of 13.7 per 100 km^2. FSF and SSM exhibited high wildfire densities, with 9.7 and 6.6 wildfires per 100 km² respectively. Although the number of hotspots in LRF (4,679 hotspots) was the highest after PSF, the density was only 1.9 hotspots per 100 km^2, which is lower than that of the freshwater swamp and mangrove ecoregions. The MRF and TPF ecoregions had the lowest density of hotspots, at 0.4 points per 100 km^2.

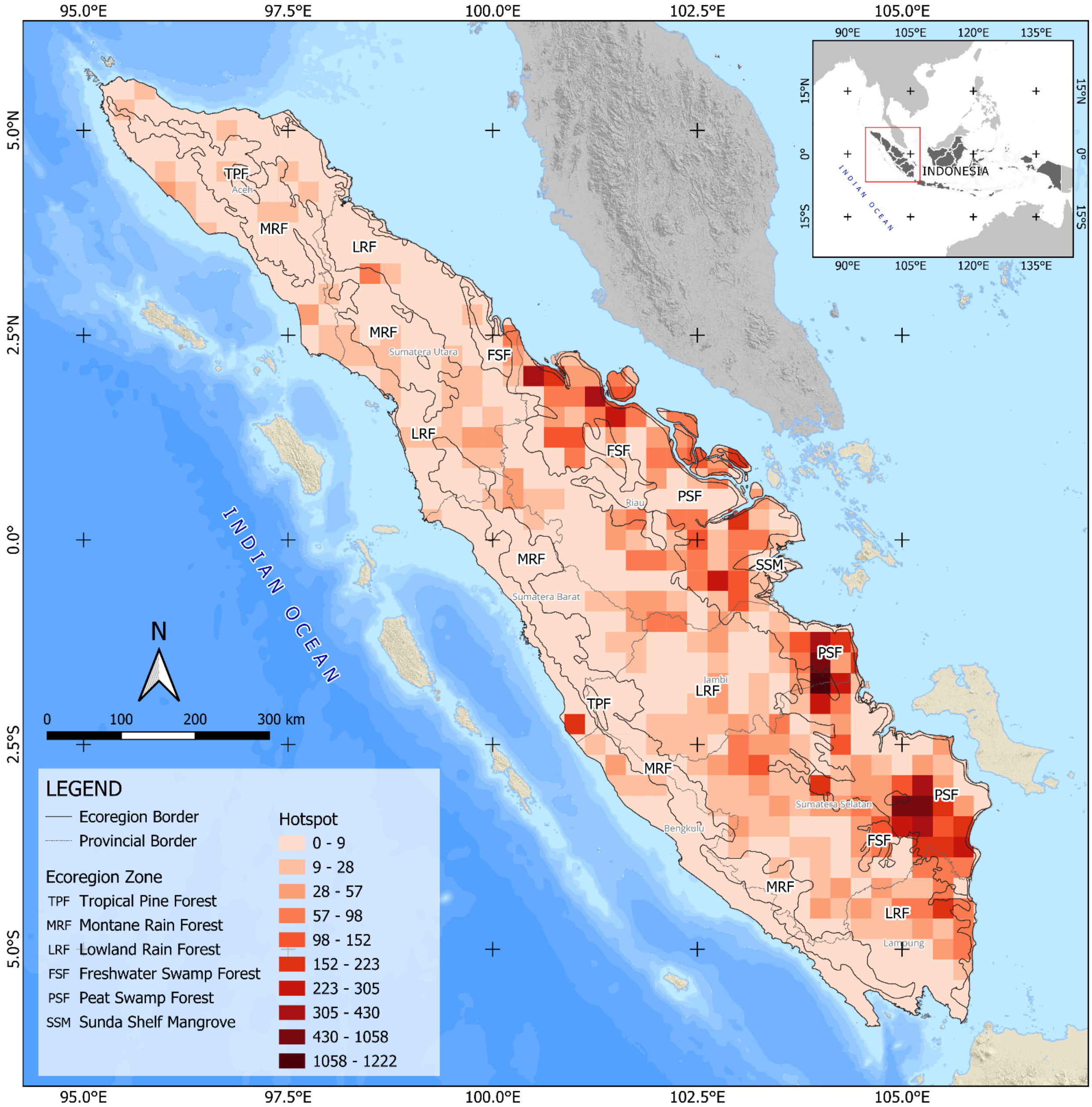

Figure 3. Sumatra Wildfire Hotspot Density Map (Source: MODIS Active Fire Data, Processed in QGIS 3.34).

The annual distribution of wildfires shown in Figure 4 indicates significant spikes in dry years, particularly 2019 (11,241 hotspots) and 2023 (2,872 hotspots). Wildfire occurrence declined markedly after 2019, with relatively lower hotspot counts recorded during the period 2020 to 2022, before increasing again in 2023. Across all years, peat swamp forests (PSFs) consistently contributed the largest proportion of hotspots, particularly during high-fire years. In addition, Figure 5 presents wildfire occurrences on the seasonal scale, which are strongly concentrated in the late dry season. Wildfire activities increased sharply in July and peaked between August and October throughout the study period. The highest monthly wildfire count was recorded in September (7,245 hotspots), followed by October (4,069 hotspots). However, wildfire occurrence remained comparatively low between December and June each year. A smaller secondary increase in hotspot activity was also observed from February to March. Similar to the annual distribution, PSF-dominated hotspot occurrence occurred during the peak wildfire months, while MRF and TPF consistently exhibited relatively low hotspot densities throughout the year.

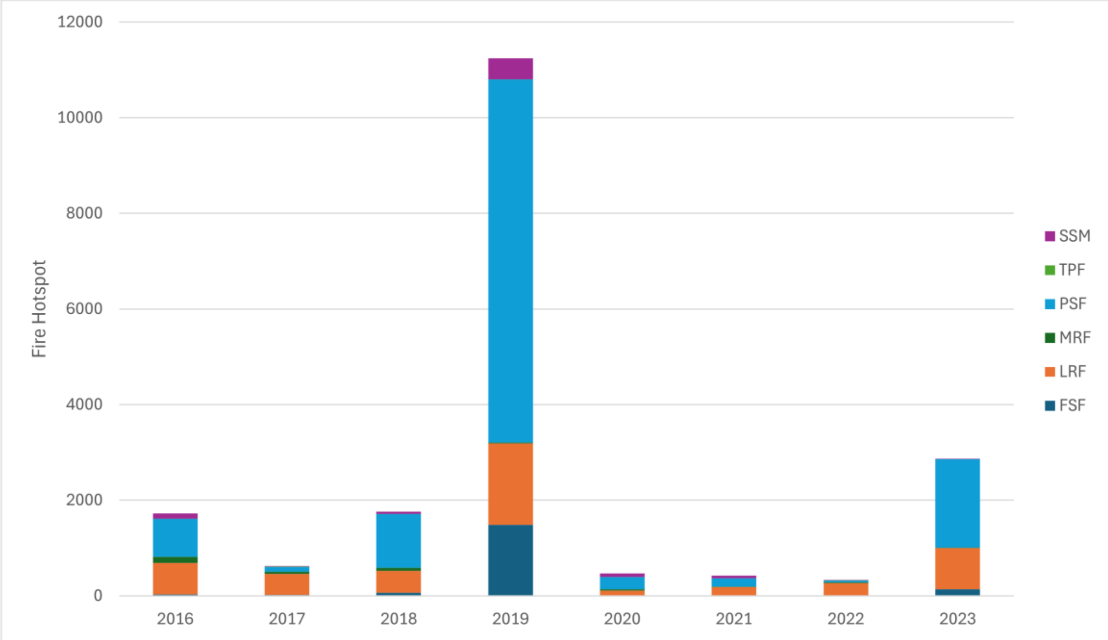

Figure 4. Annual Wildfire Hotspot Distribution Across Ecoregions in Sumatra (Source: MODIS Active Fire data).

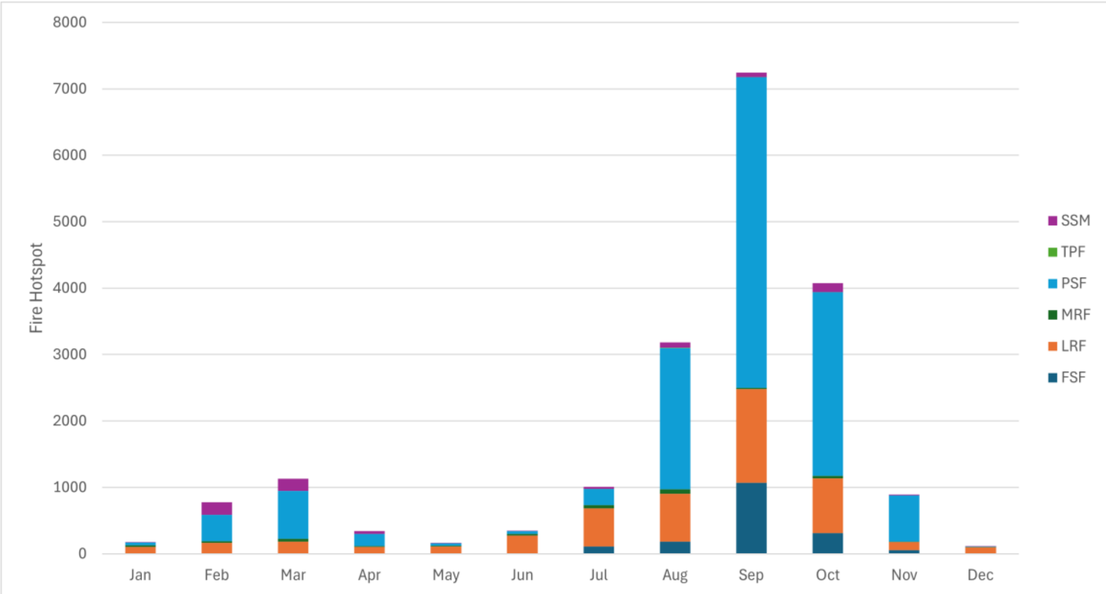

Figure 5. Monthly Wildfire Hotspot Distribution Across Ecoregions in Sumatra (Source: MODIS Active Fire Data).

3.2. Pre-fire Weather Dynamics

Pre-fire weather dynamics in shown Figure 6 demonstrate consistent patterns across ecoregions during the D−7 to D−0 period. The average decrease in rainfall over the 8 days was approximately 1.41 mm, with the decline becoming progressively more evident toward the wildfire occurrence date. Relative to the 8-day pre-fire average, most areas still exhibit positive rainfall anomalies from D-7 to D-5, particularly in the western part of Sumatra. A more pronounced decline was evident at D-4 and D-3, with mean daily rainfall anomalies across ecoregions ranging from −0.5 to 0 mm relative to the 8-day pre-fire baseline. This decreasing pattern continued across all ecoregions until D-1. Spatially, the onset of rainfall deficits occurred earlier in the eastern coastal plains, where negative anomalies were already evident at D-5, compared to the mountainous western regions. Referring to Table 1, the MRF ecoregion showed the greatest decrease in rainfall, with an average fall of 0.479 mm/day, while the FSF and PSF only experienced a decrease in rainfall of 0.071 mm/day and 0.183 mm/day. The absolute daily rainfall showed that MRF maintained the highest precipitation levels throughout the period, while FSF consistently recorded the lowest rainfall.

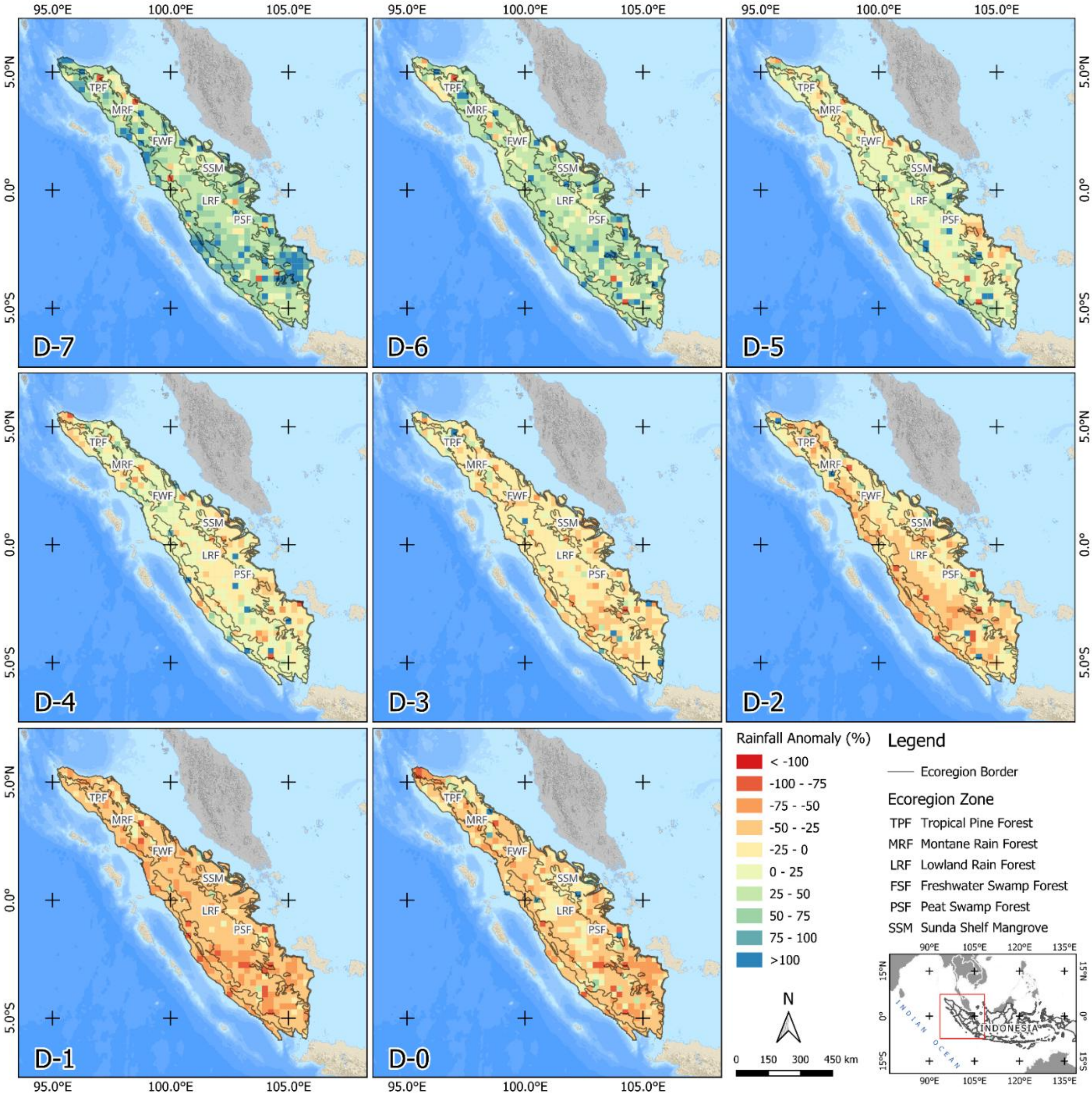

Figure 6. Pre-Fire Rainfall Dynamics Map (Source: MODIS Active Fire Data and ERA5 Total Precipitation Data, Processed in Python and QGIS 3.34).

Table 1. Pre-fire Rainfall Dynamics.

Ecoregion	Rainfall (mm)							
	D-7	D-6	D-5	D-4	D-3	D-2	D-1	D-0
FSF	1.28	1.21	1.02	0.88	1.07	1.09	0.70	0.78
LRF	3.66	3.28	2.98	2.62	2.10	1.75	1.34	1.59
MRF	5.60	5.36	3.98	3.74	3.38	2.61	2.48	2.25
PSF	2.39	2.11	1.62	1.48	1.30	1.38	0.99	1.11
TPF	2.65	2.55	0.91	1.00	1.51	0.82	0.51	0.90
SSM	3.72	3.95	3.17	2.93	2.30	2.09	1.55	2.27

FSF = freshwater swamp forest, LRF = lowland rainforest, MRF = montane rainforest, PSF = peat swamp forest, TPF = tropical pine forest, SSM = Sunda Shelf mangrove

The pre-fire temperature dynamics shown in Figure 7 indicate an increasing trend across all ecoregions, with absolute temperature values demonstrating stratification among ecoregions. FSF, MRF and TPF maintained lower temperatures, while LRF, PSF and SSM consistently exhibited higher ones. During the D-7 to D-5 period, most areas showed negative anomalies, especially in MRF and some parts of LRF, which had relatively stable pre-fire temperatures during the early observation period. The earliest and most widespread positive temperature anomaly appeared in the LRF and PSF ecoregions around D-4. Temperature increases became more evident from D-4 to D-2, with PSF recording a mean increase of 0.10°C over this 2-day interval. Meanwhile, the highest anomalies in D-1 to D-0 were more dominant in LRF. Referring to the values in Table 2, the rate of pre-fire temperature increase in PSF was comparatively lower (0.061°C/day) than in LRF (0.081°C/day), which represented a temperature rise of 0.57°C over the 7-day pre-fire window. The temperature change showed lower rates of increase in PSF (0.0610°C/day) and SSM (0.0639°C/day) than in MRF (0.0776°C/day) and TPF (0.1168°C/day). TPF, which had the highest temperature increase rate, showed an abrupt temperature increase of 0.62°C between D-2 and D-1, relative to the more gradual warming rates in other ecoregions.

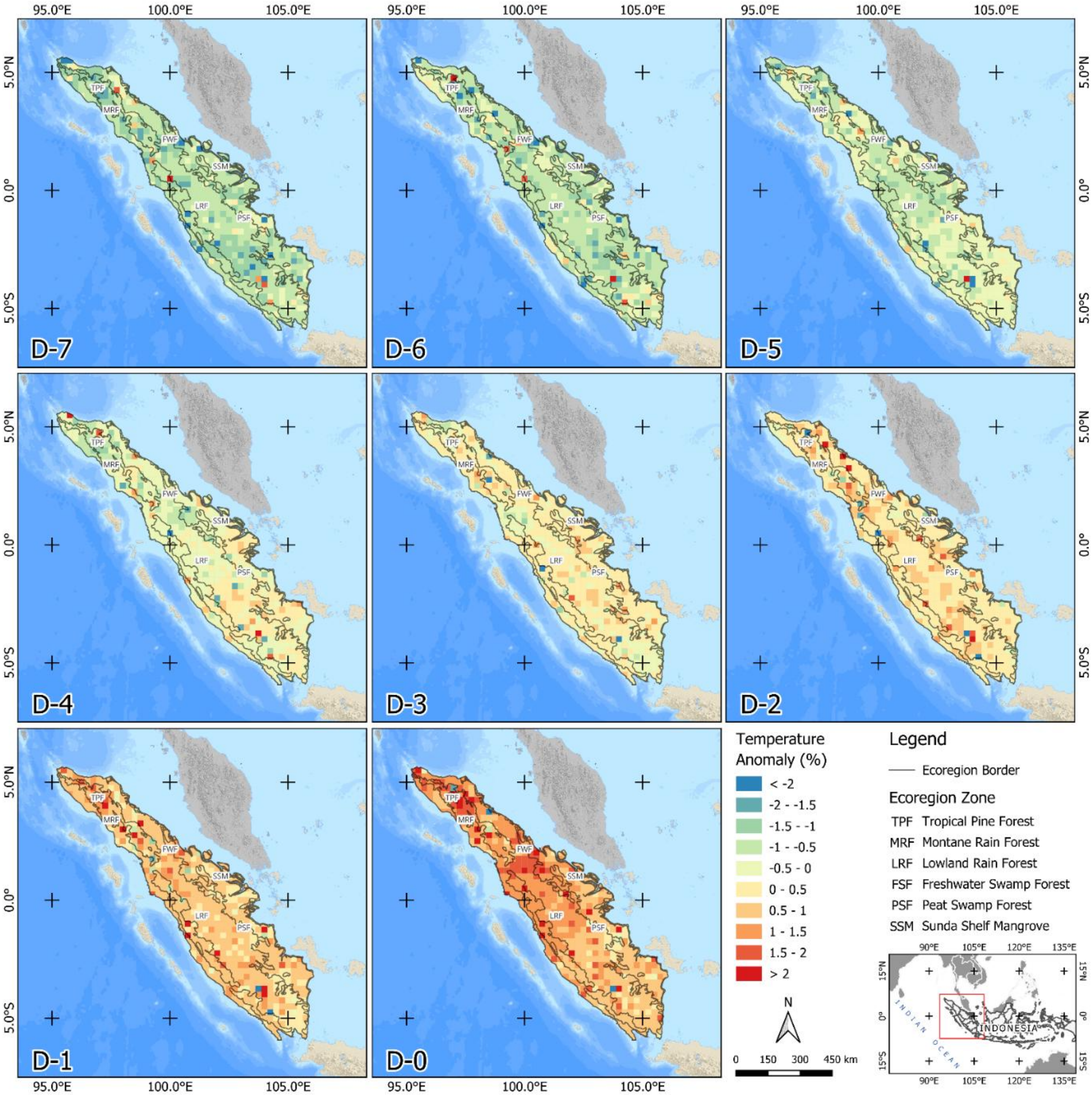

Figure 7. Pre-fire Temperature Dynamics Map (Source: MODIS Active Fire Data and ERA5 2m-temperature Data, Processed in Python and QGIS 3.34).

Table 2. Pre-fire Temperature Dynamics.

Ecoregion	Temperature (°C)							
	D-7	D-6	D-5	D-4	D-3	D-2	D-1	D-0
FSF	28.32	28.30	28.41	28.43	28.49	28.44	28.53	28.52
LRF	27.09	27.17	27.21	27.34	27.37	27.48	27.55	27.66
MRF	21.72	21.74	21.80	21.88	21.96	22.09	22.14	22.27
PSF	28.15	28.17	28.28	28.35	28.44	28.45	28.53	28.59
TPF	20.23	20.43	20.35	20.36	20.43	20.37	20.99	21.04
SSM	27.82	27.81	27.85	27.96	28.01	28.09	28.17	28.25

FSF = freshwater swamp forest, LRF = lowland rainforest, MRF = montane rainforest, PSF = peat swamp forest, TPF = tropical pine forest, SSM = Sunda Shelf mangrove.

Figure 7 shows a gradual change in pre-fire soil moisture anomalies across most areas of Sumatra. Similar to the pattern shown by rainfall, the decrease in soil moisture during the period D-7 to D-5 was not very noticeable, although significant declines became evident closer to the wildfire occurrence date. Reductions in soil moisture intensified during the D-2 to D-0 window, with the highest absolute decrease in SSM (1.07%) and FSF (0.40%). Spatially, PSF, FSF and SSM exhibited higher soil moisture declines than other ecoregions, especially in the central part. However, LRF, MRF and TPF showed more modest declines, each decreasing by less than 0.40%. The LRF ecoregion showed a modest decrease, with an average pre-fire decline of approximately 1.05%. MRF and TPF also showed comparatively modest day-to-day soil moisture changes, ranging from 0.05 to 0.17% in one day. Table 3 shows that FSF, PSF and SSM exhibited higher pre-fire soil moisture ranges of 54-55%, 65-67% and 75-77%, respectively, while the other three ecoregions exhibited similar lower soil moisture levels. Compared to the other ecoregions, swamp and mangrove ecosystems maintained higher baseline soil moisture despite experiencing noticeable short-term pre-fire declines.

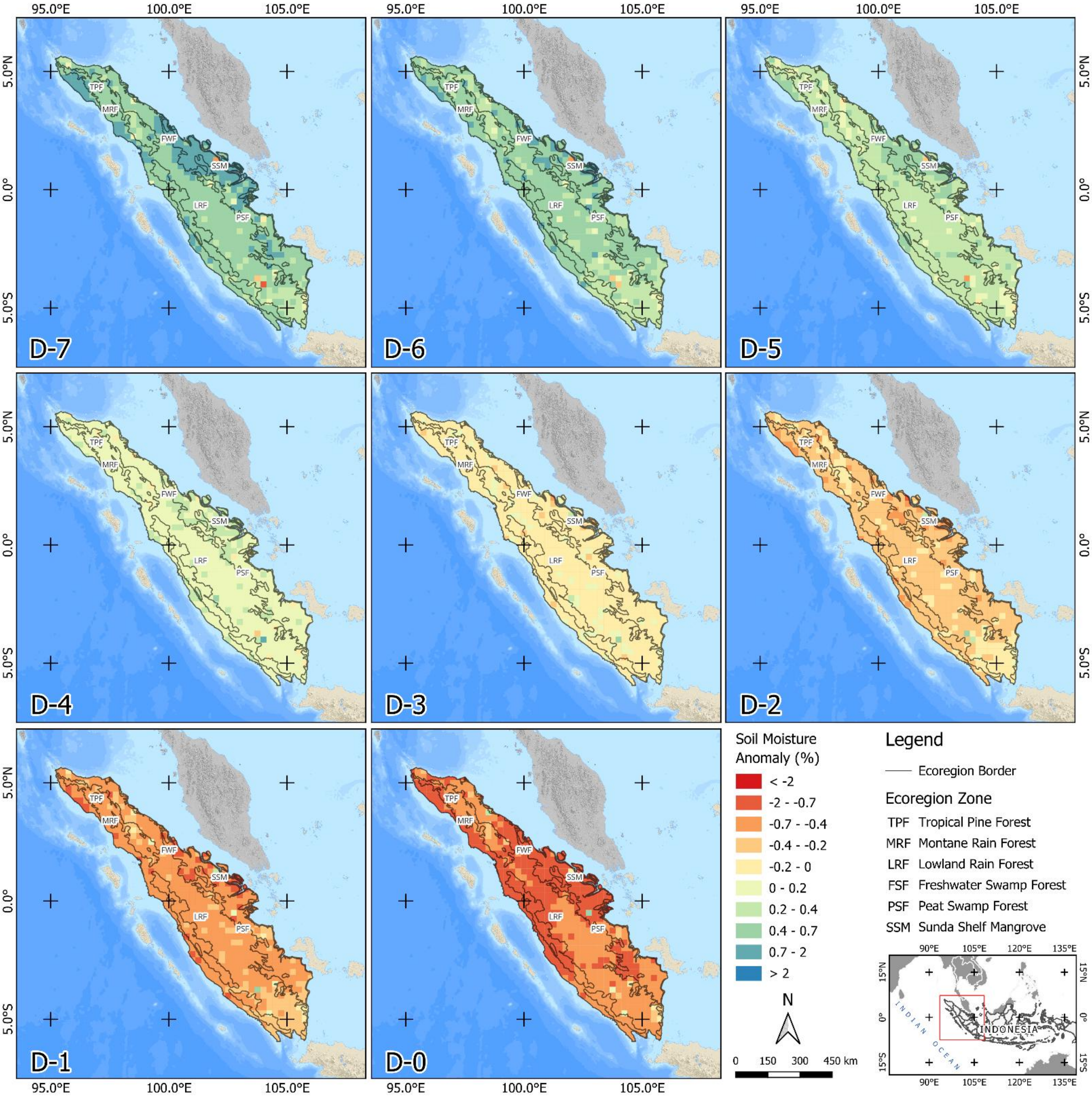

Figure 8. Pre-fire Soil Moisture Dynamics Map (Sources: MODIS Active Fire data and SMAP Soil Moisture Data Processed in Python and QGIS 3.34, 2025).

Table 3. Pre-fire Soil Moisture Dynamics.

Ecoregion	Soil Moisture (%)							
	D-7	D-6	D-5	D-4	D-3	D-2	D-1	D-0
FSF	55.62	55.46	55.30	55.15	54.99	54.84	54.64	54.44
LRF	34.81	34.72	34.63	34.50	34.33	34.14	33.94	33.76
MRF	34.03	33.98	33.86	33.74	33.64	33.49	33.32	33.17
PSF	67.05	66.92	66.73	66.54	66.32	66.10	65.88	65.62
TPF	33.64	33.35	33.17	32.97	32.84	32.78	32.57	32.37
SSM	77.06	76.92	76.71	76.43	76.14	75.78	75.42	75.07

FSF = freshwater swamp forest, LRF = lowland rainforest, MRF = montane rainforest, PSF = peat swamp forest, TPF = tropical pine forest, SSM = Sunda Shelf mangrove.

3.3. Wildfire and Weather Dynamics Linkage Based on Ecoregion

Negative binomial regression was applied to quantify the weather–wildfire relationship across ecoregions. The dispersion parameter (α) was greater than zero and statistically significant ($\alpha = 0.7184$, $p < 0.05$), which confirmed the presence of overdispersion and the appropriateness of this specification over Poisson regression. The relationship between the number of hotspots and rainfall, temperature and soil moisture, as presented in Table 4, shows varying results between ecoregions. The strongest relationship was shown by the FSF ecoregion, where the full model yielded the highest pseudo-R^2 (0.226), indicating the greatest improvement in model fit. Comparatively moderate fit improvements were observed in SSM (pseudo-R^2 = 0.140) and PSF (pseudo-R^2 = 0.052). Weaker fit improvement by weather variables was observed in LRF (pseudo-R^2 = 0.019) and in the combined MRF and TPF (pseudo-R^2 = 0.004). The coefficients of rainfall, temperature and soil moisture showed significant effects overall. However, there were variations in the effect with different levels of significance, both between ecoregions and between variables. In LRF and PSF, which had the largest number of wildfire hotspots, rainfall and temperature variables showed significant associations, while the soil moisture variable did not, demonstrating a significant statistical association in FSF and SSM instead. However, the effect was relatively modest, with a 1% increase in soil moisture contributing to a 1.97% increase in the expected incidence rate of wildfire hotspots in FSF and 3.41% in SSM. MRF and TPF exhibited no significant coefficients for any of the three weather variables.

The IRR values show that a 1 mm increase in rainfall was associated with a 3.52% lower expected incidence rate of wildfire hotspots in LRF (IRR = 0.965) and a 10.35% lower expected incidence rate in PSF (IRR = 0.897). Meanwhile, a 1°C increase in temperature was associated with a 6.19% higher expected incidence rate of wildfire hotspots in LRF (IRR = 1.062) and an 11.45% higher rate in PSF (IRR = 1.115). The rainfall variable yielded a statistically significant coefficient in FSF, with the largest effect magnitude observed across all ecoregions. A 1 mm increase in rainfall was associated with a 13.52% lower expected incidence rate of wildfire hotspots in this ecoregion (IRR = 0.865). Temperature showed a strong association with wildfire occurrence in the SSM ecoregion, with an IRR value of 1.971. This indicates that a 1°C increase in temperature was associated with a 97.1% higher expected incidence rate of wildfire hotspots. However, this magnitude must be interpreted with caution, as the observed pre-fire temperature range in SSM spanned only approximately 0.43°C across the 7-day pre-fire window.

Table 4. Negative Binomial Regression Result.

Ecoregion	No. Obs	psd. R^2	Coefficient			IRR		
			rf	tm	sm	rf	tm	sm
FSF	402	0.226	-0.145*	0.056	0.020*	0.865*	1.058	1.020*
LRF	2670	0.019	-0.036*	0.060*	0.002	0.965*	1.062*	1.002
MRF & TPF	229	0.004	0.006	-0.006	0.013	1.006	0.994	1.013
PSF	2344	0.052	-0.109*	0.108*	0.001	0.897*	1.115*	1.001
SSM	216	0.140	-0.036	0.679*	0.034*	0.965	1.971*	1.034*
All	5548	0.166	-0.089*	0.109*	0.013*	0.915*	1.115*	1.014*

FSF = freshwater swamp forest, LRF = lowland rainforest, MRF = montane rainforest, PSF = peat swamp forest, TPF = tropical pine forest, SSM = Sunda Shelf mangrove, No. Obs = number of observations, psd. R^2 = pseudo-R^2, IRR = Incidence Rate Ratio, rf = rainfall, tm = temperature, sm = soil moisture
**Statistical significance at $p < 0.05$.*

4. Discussion

Our spatiotemporal analysis of wildfire dynamics across Sumatra reveals that the relationship between short-term weather variability and wildfire occurrence is strongly mediated by ecoregional characteristics, particularly hydrological conditions, ecosystem structure, and landscape disturbance. The spatial difference of wildfire concentration between FSF, PSF and SSM with LRF, MRF and TPF was consistent with recent global results showing that swamp and mangrove ecosystems are increasingly prone to wildfires due to hydrological disturbance, including altered water balance and vegetation stress associated with coastal drying during prolonged dry seasons (Chen & Liu, 2024; O *et al.,* 2020). Wildfire vulnerability is further intensified by the land-use conversion, peat drainage and deforestation associated with resource exploitation (Eddy *et al.,* 2021). These anthropogenic disturbances also increase the sensitivity of tropical ecosystems to short-term weather anomalies by altering hydrological conditions, lowering water tables, and increasing fuel flammability during dry periods (Salmayenti *et al.,* 2025; Taufik *et al.,* 2022). Although anthropogenic variables were not included in this study, the observed weather–wildfire relationships must be interpreted within the broader context of human-modified landscapes. For instance, the low density of hotspots in MRF and TPF suggests that these ecosystems are relatively more resistant to wildfire occurrence and less exposed to anthropogenic ignition pressures. This pattern can be seen in the mountainous topography of western Sumatra, with limited human disturbance and wildfire exposure (Avcıoğlu *et al.,* 2024). However, the reduced wildfire frequency in these highland ecosystems does not necessarily imply immunity. A study of tropical montane zones by Swann *et al.* (2023) revealed that rising temperatures and precipitation shifts were extending wildfire seasons and altering wildfire boundaries, even in these stable ecosystems.

Temporally, the extreme wildfire years were consistent with large-scale ENSO–IOD influences referred to in the introduction. During El Niño events, suppressed rainfall prolongs dry season conditions into September–November, delaying fuel rewetting and extending the wildfire-prone period. The seasonal pattern of wildfired indicated that wildfire activity intensifies after the climatological peak of the dry season (June–August) in both equatorial and monsoonal climates. This seasonal pattern also shows the differing climatic regimes across Sumatra, in which the lower hotspot peak during February–March corresponds to the first dry season in equatorial climate regions. Meanwhile, the delayed responses of wildfire activity are consistent with a recent tropical study showing an inverse relationship between precipitation and wildfire occurrence, suggesting a time-lagged response of wildfire activity to rainfall and fuel drying conditions (Li *et al.,* 2025).

The observed pre-fire weather dynamics consistently revealed a difference between coastal lowland and upland ecosystems. Coastal swamp ecoregions remain vulnerable to wildfire even under modest rainfall deficits, likely due to the rapid increase in fuel flammability associated with organic-rich surface layers and shallow water-table responses (Irfan *et al.,* 2021). On the other hand, mountainous areas experience higher rainfall that buffer them against short-term moisture stress. This pattern is similar to that of other humid tropical regions, where orographic precipitation and lower vapor pressure deficits confer greater climatic resilience (Lafon & Quiring, 2012; Petrov *et al.,* 2023). Temperature dynamics show a similar ecoregional contrast, including the progressive pre-fire warming observed across all ecoregions, consistent with global evidence that elevated temperatures increase the probability of ignition (Ma *et al.,* 2024). Meanwhile, the persistent thermal stratification, with FSF, PSF and SSM maintaining higher temperatures than MRF and TPF, reflect their contrasting latitudinal and elevational positions. In dense, moisture-rich tropical ecosystems, temperature effects are often manifested indirectly through enhanced evapotranspiration, atmospheric drying and reductions in canopy fuel moisture (O'Donnell *et al.,* 2011). Together, these atmospheric differences show that hydrologically-sensitive coastal ecosystems respond rapidly to short-term atmospheric drying than upland forest systems (Flannigan *et al.,* 2015).

While rainfall and temperature primarily represent short-term atmospheric variability, soil moisture provides a more direct representation of hydrological conditions related to fuel availability and combustion persistence. The 7-day average soil moisture could not fully capture threshold-based or lagged hydrological effects underlying the abrupt ignition processes associated with critical moisture thresholds. However, such soil moisture deficits still reflect ignition potential and influence wildfire severity through their effect on fuel continuity and combustion completeness (Pulla *et al.,* 2016). In swamp-dominated regions with a high soil moisture baseline, a 5% decline corresponds to an exponential increase in smouldering depth and the overall hotspot number (Brasika, 2022). Notably, ecoregions that exhibited larger pre-fire soil moisture declines, such as FSF, PSF and SSM, were also those with the highest hotspot densities. In these ecosystems, wildfire susceptibility is more appropriately understood as a function of relative drying from normally saturated baseline conditions, rather than of absolute moisture levels (Azmi *et al.,* 2025; Taufik *et al.,* 2022). This mechanism explains the counterintuitive positive coefficients of soil moisture in FSF and SSM. Although the negative binomial regression identified statistically significant associations, the corresponding IRR indicated relatively small changes (less than 5%), suggesting that soil moisture influences wildfire in a nonlinear and potentially threshold-based manner. The regression analysis quantitatively supported the descriptive spatiotemporal patterns observed across the six ecoregions, across which the Pseudo-R^2 values were relatively modest, indicating that the regression models captured only limited improvements in fit relative to null models within this complex wildfire system. The values suggest that meteorological variability alone accounted for only a proportion of the observed variation in wildfire occurrence, consistent with previous findings on tropical ecosystems, indicating that weather variables function more as short-term enabling conditions than as sole determinants of wildfire activity (Pacuk *et al.,* 2025).

The ecoregion-specific regression coefficients and IRR values quantitatively demonstrated significant differences in wildfire sensitivity between ecosystems. The results were consistent with previous studies showing that the relationship between rainfall and wildfire activity in humid tropical regions is highly nonlinear, where even short rainfall events rapidly suppress wildfire spread in swamp ecosystems (Mishra & Singh, 2010). Similarly, Schaefer and& Magi (2019)demonstrated that the sensitivity of wildfire occurrence to rainfall was particularly pronounced in areas with shallow water tables and organic-rich soils, such as FSF and PSF. The relatively large IRR associated with temperature in SSM was consistent with recent observations in coastal tropical environments, in which canopy structure and salt exposure were shown to intensify surface drying under warmer conditions (Dookie *et al.,* 2025).

The absence of significant coefficients in MRF and TPF was consistent with results from Petrov *et al.* (2023), indicating that montane and coniferous ecosystems typically exhibited higher climatic buffering due to lower human ignition pressure and more stable moisture regimes. Therefore, the weak weather sensitivity in these high-elevation systems demonstrates both ecological resistance and limited anthropogenic exposure. The difference between highly sensitive coastal ecosystems and comparatively stable upland systems emphasizes the importance of ecoregion-specific climatic thresholds in shaping wildfire susceptibility across Sumatra. In addition, rainfall and temperature were associated with short-term atmospheric conditions linked to wildfire occurrence, while soil moisture showed broader hydrological constraints on sustained combustion. The results emphasize that wildfire vulnerability in tropical landscapes is strongly conditioned by the interaction between short-term weather variability, hydrological sensitivity, and ecosystem-specific landscape characteristics.

5. Conclusion

In conclusion, the study demonstrates that wildfire vulnerability in tropical landscapes is strongly differentiated by ecosystem type, with coastal wetland systems exhibiting the greatest sensitivity to short-term hydrometeorological variability. Reduced rainfall and elevated temperatures are consistently associated with increased wildfire occurrence, particularly in carbon-rich peatland and mangrove ecosystems. These results reinforce growing evidence from recent tropical wildfire studies that degraded tropical wetlands are highly sensitive to short-term hydrometeorological fluctuations. As climate change intensifies, the risk of recurrent wildfire in these ecosystems escalates, not only in Sumatra, but also across humid tropical regions. Recognizing ecoregion-specific responses to weather variability is essential for improving fire danger forecasting, early warning systems, and regionally targeted wildfire mitigation policies.

Unlike many previous tropical wildfire studies that have focused primarily on peatlands or seasonal drought conditions, the integration of weather sensitivity into ecoregion-based wildfire assessment in this study demonstrates that weather–wildfire relationships vary significantly across ecoregions and are strongly mediated by ecosystem-specific hydrological characteristics. This can improve the spatial prioritization of wildfire prevention efforts applied to tropical landscapes and coastal ecosystems. From a practical perspective, the findings offer valuable insights to support environmental agencies and policymakers in identifying ecosystems that require more intensive hydrological monitoring and wildfire prevention during drought periods. However, the study is limited by its reliance on moderate-resolution satellite data and the use of relatively simple meteorological variables. Future studies should integrate finer-scale climate, hydrological, land-use and anthropogenic datasets to better capture the interactions between weather variability, ecosystem disturbance, and human-driven wildfire processes. The development of a comprehensive wildfire model could improve predictive capabilities and strengthen adaptation strategies in a changing climate.

Acknowledgements

The authors gratefully acknowledge the financial support provided by Universitas Gadjah Mada through the Final Project Recognition Grant (*Rekognisi Tugas Akhir*) in 2024.

Author Contributions

Conceptualization: Asshaffa Naim, Andung Bayu Sekaranom; **methodology**: Asshaffa Naim; **investigation**: Asshaffa Naim; **writing—original draft preparation**: Asshaffa Naim; **writing—review and editing**: Andung Bayu Sekaranom, Sudrajat, Fitria Nucifera; **visualization**: Asshaffa Naim. All authors have read and agreed to the published version of the manuscript.

Conflict of interest

All authors declare that they have no conflicts of interest.

Data availability

Data are available upon request.

Funding

This research was supported by a Grant of Final Project Recognition (Rekognisi Tugas Akhir) by Universitas Gadjah Mada in 2024. The grant was entitled "Analisis Dampak Perubahan Iklim terhadap Kerentanan dan Ketahanan Lingkungan Lokal di Indonesia" with Dr. Sc. Andung Bayu Sekaranom, M.Sc. as the lead researcher (Contract Number: 5286/UN1.P1/PT.01.03/2024 in May 6th 2024).

References

Arias-Muñoz, P., Cabrera-García, S., & G., J.-A. (2024). A Multicriteria Geographic Information System analysis of wildfire susceptibility in the ANDEAN region: a case study in Ibarra, Ecuador. *Fire,* 7(3), 81. doi: 10.3390/fire7030081

Ariska, M., Suhadi Irfan M., S., & I., I. (2024). Detection of Dominant Rainfall Patterns in Indonesian Regions Using Empirical Orthogonal Function (EOF) and Its Relation with ENSO and IOD Events. *Science & Technology Indonesia,* 9(4), 1009–1023. doi: 10.26554/sti.2024.9.4.1009-1023

Avcıoğlu, A., Akbaş, A., Görüm, T., & Ö., Y. (2024). The compound effect of topography, weather, and fuel type on the spread and severity of the largest wildfire in NW of Turkey. Natural Hazards, 121, 3219–3237. doi: 10.1007/s11069-024-06885-7

Azmi, N. A. C., Rashid, A. S. A., Apandi, N. M., Rasib A W and Nasir, M. N. M., Zainorabidin, A., Mohamed, M. S., Shah, M. A. M., Lat, D. C., & Ismail, A. (2025). Comprehensive investigation of the smouldering characteristics of hemic peat under varying moisture conditions and the combined influence of wind velocity and direction. Phys. Chem. *Earth Parts A/B/C,* 140, 104054. doi: 10.1016/j.pce.2025.104054

Brasika, I. B. M. (2022). The role of El Nino variability and Peatland in burnt area and emitted carbon in forest fire modeling. *Forest and Society,* 84–103. doi: 10.24259/fs.v6i1.10671

Briones-Herrera, C. I., Vega-Nieva, D. J., Monjarás-Vega, N. A., Briseño-Reyes, J., López-Serrano, P. M., Corral-Rivas, J. J., Alvarado-Celestino, E., Arellano-Pérez, S., Álvarez-González, J. G., Ruiz-González, A. D., Jolly, W. M., & S. A., P. (2020). Near Real-Time Automated Early Mapping of the Perimeter of Large Forest Fires from the Aggregation of VIIRS and MODIS Active Fires in Mexico. *Remote Sensing,* 12(12), 2061. doi: 10.3390/rs12122061

Chen, H., & Liu, F. (2024). Soil depth and recovery interval mediate soil water repellency under different forest types and fire intensity levels in China: Evidence for ecosystem resiliency. *Soil and Tillage Research,* 237, 105982. doi: 10.1016/j.still.2023.105982

Cho, Y., Yoon, J., Jeong, J., Kug, J., Kim, B., Kim, H., Park, R. J., & S., K. (2024). Precipitation-induced abrupt decrease of Siberian wildfire in summer 2022 under continued warming. Environmental Research Letters, 19(7), 074037. doi: 10.1088/1748-9326/ad5573

Chowdhury, E., & Hassan, Q. (2015). Development of a New Daily-Scale Forest Fire Danger Forecasting System Using Remote Sensing Data. *Remote Sensing,* 7(3), 2431–2448. doi: 10.3390/rs70302431

Curcan, G., Drăguleasa, I.-A., & I. E., M. (2023). Practical model of climate variability and vegetation distribution in the Oltenia Plain. Oltenia. Studii Și Comunicări. *Științele Naturii,* 39(1), 272–273.

Dinerstein, E., Olson, D., Joshi, A., Vynne, C., Burgess, N. D., Wikramanayake, E., Hahn, N., Palminteri, S., Hedao, P., Noss, R., Hansen, M., Locke, H., Ellis, E. C., Jones, B., Barber, C. V., Hayes, R., Kormos, C., Martin, V., Crist, E., … Saleem, M. (2017). An ecoregion-based approach to protecting half the terrestrial realm. *Bioscience*, 67(6), 534–545.

Dookie, S., Ansari, A. A., & Jaikishun, S. (2025). Forest-fire interactions, impacts, and implications: a focus on mangroves. *New Zealand Journal of Forestry Science,* 55. doi: 10.33494/nzjfs552025x405x

Drăguleasa, I., Niță, A., Mazilu, M., & G., C. (2023). Spatio-Temporal distribution and trends of major agri-cultural crops in Romania using interactive geographic Information system mapping. *Sustainability,* 15(20), 14793. doi: 10.3390/su152014793

Eddy, S., Milantara, N., Sasmito, S. D., Kajita, T., & M., B. (2021). Anthropogenic drivers of mangrove loss and associated carbon emissions in South Sumatra, Indonesia. *Forests,* 12(2), 187. doi: 10.3390/f12020187

Flannigan, M. D., Wotton, B. M., Marshall, G. A., De Groot, W. J., Johnston, J., Jurko, N., & Cantin, A. S. (2015). Fuel moisture sensitivity to temperature and precipitation: climate change implications. *Climatic Change,* 134(1–2), 59–71. doi: 10.1007/s10584-015-1521-0

Giglio, L., Schroeder, W., & Justice, C. O. (2016). The collection 6 MODIS active fire detection algorithm and fire products. *Remote Sensing of Environment,* 178, 31–41. doi: 10.1016/j.rse.2016.02.054

Gincheva, A., Pausas, J. G., Torres-Vázquez, M. N., Bedia, J., Vicente-Serrano, S. M., Abatzoglou, J. T., Sánchez-Espigares, J. A., Chuvieco, E., Jerez, S., Provenzale, A., Trigo, R. M., & M., T. (2024). The Interannual Variability of Global Burned Area Is Mostly Explained by Climatic Drivers. *Earth S Future,* 12(7). doi: 10.1029/2023ef004334

Hayasaka, H. (2023). Fire Weather Conditions in Plantation Areas in Northern Sumatra, Indonesia. *Atmosphere,* 14(10), 1480. doi: 10.3390/atmos14101480

Hersbach, H., Bell, B., Berrisford, P., Biavati, G., Horányi, A., Muñoz Sabater, J., Nicolas, J., Peubey, C., Radu, R., Rozum, I., Schepers, D., Simmons, A., Soci, C., Dee, D., & J. N., T. (2023). *ERA5 hourly data on sin-gle levels from 1940 to present [Dataset].* In Copernicus Climate Change Service (C3S) Climate Data Store (CDS). ECMWF. doi: 10.24381/cds.adbb2d47

Irfan, M., Virgo, F., Khakim, M. Y. N., Ariani, M., Sulaiman, A., & I., I. (2021). The dynamics of rainfall and temperature on peatland in South Sumatra during the 2019 extreme dry season. *Journal of Physics Conference Series*, 1940(1), 012030. doi: 10.1088/1742-6596/1940/1/012030

Justino, F., Bromwich, D. H., Wang, S., Althoff, D., Schumacher, V., & A., D. S. (2023). Influence of local scale and oceanic teleconnections on regional fire danger and wildfire trends. *The Science of the Total Environment*, 883, 163397. doi: 10.1016/j.scitotenv.2023.163397

Kementerian Kehutanan. (2025). Indikasi Luas Kebakaran Hutan dan Lahan (Ha) per Provinsi di Indonesia. Retrieved From https://sipongi.menlhk.go.id/indikasi-luas-kebakaran

Krueger, E. S., Levi, M. R., Achieng, K. O., Bolten, J. D., Carlson, J. D., Coops, N. C., Holden, Z. A., Magi, B. I., Rigden, A. J., & T. E., O. (2022). Using soil moisture information to better understand and predict wildfire danger: a review of recent developments and outstanding questions. *International Journal of Wildland Fire,* 32(2), 111–132. doi: 10.1071/wf22056

Lafon, C. W., & S. M., Q. (2012). Relationships of Fire and Precipitation Regimes in Temperate Forests of the Eastern United States. *Earth Interactions,* 16(11), 1–15. doi: 10.1175/2012ei000442.1

Li, P., Jin, X., & Li, X. (2025). How do tropical active fires respond to intra-annual climate change in the early 21st century? *Geography and Sustainability,* 6(3), 100253.

Liu, J., Wang, Y., Guo, H., Lu, Y., Xu, Y., Sun, Y., Gan, W., Sun, R., & Li, Z. (2024). Spatial and temporal patterns and driving factors of forest fires based on an optimal parameter-based geographic detector in the Panxi region, Southwest China. *Fire Ecology,* 20(1), 27. doi: 10.1186/s42408-024-00257-z

Ma, B., Liu, X., Tong, Z., Zhang, J., & X., W. (2024). Coupled effects of high temperatures and droughts on forest fires in northeast China. *Remote Sensing,* 16(20), 3784. doi: 10.3390/rs16203784

Măcețeanu, D. M., Crețan, R., Drăguleasa, I., Niță, A., & M., F. (2026). The use of GIS techniques for land use in a South Carpathian River Basin—Case study: Pesceana River Basin, Romania. *Sustainability*, 18(2), 1134. doi: 10.3390/su18021134

Mishra, A. K., & Singh, V. P. (2010). A review of drought concepts. *Journal of Hydrology,* 391(1–2), 202–216. doi: 10.1016/J.JHYDROL.2010.07.012

Moradi, A., & Rahmati, S. (2023). Ecoregional planning: An overview of concepts and approaches. Curr. *Urban Stud.,* 11(04), 682–707.

Nolan, R. H., Blackman, C. J., de Dios, V. R., Choat, B., Medlyn, B. E., Li Ximeng and Bradstock, R. A., & Boer, M. M. (2020). Linking forest flammability and plant vulnerability to drought. *Forests,* 11(7), 779.

Novitasari, N., Sujono, J., Harto, S., Maas, A., & R., J. (2019). Drought index for Peatland wildfire manage-ment in Central Kalimantan, Indonesia during El Niño phenomenon. *Journal of Disaster Research,* 14(7), 939–948. doi: 10.20965/jdr.2019.p0939

Nurdiati, S., Sopaheluwakan, A., & P., S. (2022). Joint Pattern Analysis of Forest Fire and Drought Indi-cators in Southeast Asia Associated with ENSO and IOD. *Atmosphere,* 13(8), 1198. doi: 10.3390/atmos13081198

O, S., Hou, X., & R., O. (2020). Observational evidence of wildfire-promoting soil moisture anomalies. *Scientific Reports,* 10(1). doi: 10.1038/s41598-020-67530-4

O'Donnell, A. J., Boer, M. M., McCaw, W. L., & P. F., G. (2011). Climatic anomalies drive wildfire occur-rence and extent in semi-arid shrublands and woodlands of southwest Australia. *Ecosphere,* 2(11), art127. doi: 10.1890/es11-00189.1

Pacuk, D., Van Der Sleen, P., Sterck, F. J., & M. T., V. D. S. (2025). *Toward a functional understanding of novel fire regimes in tropical forests. American Journal of Botany.* Retrieved From https://doi.org/10.1002/ajb2.70112

Petrov, I. A., Shushpanov, A. S., Golyukov, A. S., Dvinskaya, M. L., & V. I., K. (2023). Wildfire dynamics in pine forests of central Siberia in a changing climate. *Contemporary Problems of Ecology,* 16(1), 36–46. doi: 10.1134/s1995425523010067

Piza, E. L. (2012). *Using Poisson and Negative Binomial Regression Models to Measure the Influence of Risk on Crime Incident Counts. Rutgers Center on Public Security, 1–4.* Retrieved From http://rut-gerscps.weebly.com/uploads/2/7/3/7/27370595/countregressionmodels.pdf

Prasetyo, L. B., Setiawan, Y., Condro, A. A., Kustiyo, K., Putra, E. I., Hayati, N., Wijayanto, A. K., Ramadhi, A., & D., M. (2022). Assessing Sumatran Peat Vulnerability to Fire under Various Condition of EN-SO Phases Using Ma-chine Learning Approaches. *Forests,* 13(6), 828. doi: 10.3390/f13060828

Pulla, S., Riotte, J., Suresh, H. S., Dattaraja, H. S., & R., S. (2016). Controls of soil spatial variability in a dry tropical forest. *PLoS ONE,* 11(4), e0153212. doi: 10.1371/journal.pone.0153212

Quan, X., Wang, W., Xie, Q., He, B., De Dios, V. R., Yebra, M., Jiao, M., & R., C. (2023). Improving wildfire occurrence modelling by integrating time-series features of weather and fuel moisture content. *Environmental Modelling & Software,* 170, 105840. doi: 10.1016/j.envsoft.2023.105840

Reichle, R. H., De Lannoy, G., Koster, R. D., Crow, W. T., Kimball, J. S., Liu, Q., & M., B. (2022). *SPL4SMGP.007 SMAP L4 Global 9-km Surface and Root Zone Soil Moisture [Dataset].* In NASA National Snow and Ice Data Center Distributed Active Archive Center.

Ritung., S, Wahyunto K., N., & Sukarman Suparto Tafakresnanto C., H. (2018). *Peta Lahan Gambut Indonesia Skala 1:250.000.* IAARD Press.

Sabljić, L., Bajić, D., Marković, S. B., Adžić, D., Spalevic, V., Sestraş, P., Pavić, D., & T., L. (2026). Remote sens-ing and GIS assessment of drought dynamics in the Ukrina River Basin, Bosnia and Herzegovina. *Atmosphere,* 17(2), 124. doi: 10.3390/atmos17020124

Salmayenti, R., Baird, A. J., Holden, J., & D. V., S. (2025). Drainage density and land cover interact to affect fire occur-rence in Indonesian peatlands. Environmental Research Letters, 20(5), 054036. doi: 10.1088/1748-9326/adc755

Schaefer, A. J., & Magi, B. I. (2019). Land-Cover Dependent Relationships between Fire and Soil Moisture. *Fire*, 2(4), 55. doi: 10.3390/fire2040055

Stoklosa, J., Blakey, R. V, & F. K. C., H. (2022). An overview of modern applications of negative binomial mod-elling in ecology and Biodiversity. *Diversity,* 14(5), 320. doi: 10.3390/d14050320

Swann, D. E. B., Bellingham, P. J., & Martin, P. H. (2023). Resilience of a tropical montane pine forest to fire and severe droughts. *Journal of Ecology,* 111(1), 90–109. doi: 10.1111/1365-2745.14017

Syaufina, L., Darojat, S. N., Sitanggang, I. S., & N., A. (2018). Forest fire as a threat for biodiversity and urban pollution. *IOP Conference Series Earth and Environmental Science,* 203, 012015. doi: 10.1088/1755-1315/203/1/012015

Taufik, M., Widyastuti, M. T., Sulaiman, A., Murdiyarso, D., Santikayasa, I. P., & B., M. (2022). An im-proved drought-fire assessment for managing fire risks in tropical peatlands. *Agricultural and Forest Meteorology*, 312, 108738. doi: 10.1016/j.agrformet.2021.108738

Wasserman, T. N., & Mueller, S. E. (2023). Climate influences on future fire severity: a synthesis of climate-fire interac-tions and impacts on fire regimes, high-severity fire, and forests in the western United States. *Fire Ecology,* 19(1), 43. doi: 10.1186/s42408-023-00200-8

Abbreviations

TPF	Tropical Pine Forest
MRF	Montane Rain Forests
LRF	Lowland Rain Forests
FSF	Freshwater Swamp Forests
PSF	Peat Swamp Forests
SSM	Sunda Shelf Mangroves
No. Obs	number of observation
psd. R2	pseudo-R2
rf	rainfall
tm	temperature
sm	soil moisture